# Hydrogen-terminated defects in ion-implanted silicon probed by monoenergetic positron beams

Akira Uedono, Toshiki Mori, Kunitomo Morisawa, and Kouichi Murakami
*Institute of Applied Physics, University of Tsukuba, Tsukuba, Ibaraki 305-8573, Japan*

Toshiyuki Ohdaira, Ryoichi Suzuki, and Tomohisa Mikado
*National Institute of Advanced Industrial Science and Technology, Tsukuba, Ibaraki 305-8568, Japan*

Kunie Ishioka and Masahiro Kitajima
*Material Engineering Laboratory, National Institute for Materials Science, Tsukuba, Ibaraki 305-0047, Japan*

Shunichi Hishita, Hajime Haneda, and Isao Sakaguchi
*Advanced Materials Laboratory, National Institute for Materials Science, Tsukuba, Ibaraki 305-0044, Japan*

(Received 18 July 2002; accepted 6 December 2002)

Hydrogen-terminated vacancies in $Si^+$-implanted Si were studied by means of positron annihilation. After the $Si^+$-ion implantation, hydrogen atoms were introduced into the damaged region using a hydrogen plasma [hydrogen-atom treatment (HAT)]. Monoenergetic positron beams were used to measure Doppler broadening spectra of the annihilation radiation and the lifetime spectra of positrons. It was found that the line shape parameter, *S*, corresponding to the annihilation of positrons trapped by vacancy-type defects, decreased after HAT. This was attributed to the trapping of positrons by H-decorated vacancy-type defects. Isochronal annealing experiments revealed a strong correlation between positron annihilation parameters and Raman intensities of Si–H, suggesting that hydrogen atoms are released from vacancy-type defects after annealing at 600 °C.
© *2003 American Institute of Physics.* [DOI: 10.1063/1.1542923]

## I. INTRODUCTION

It is important to study the behavior of hydrogen in Si because it affects the electrical properties of Si devices.[1] During the processing steps of semiconductor devices, Si wafers interact with a large amount of hydrogen. For example, bond-and-etch-back processes used in the fabrication of silicon-on-insulator wafers involve implantation of high doses of hydrogen or annealing in hydrogen atmosphere.[2,3] Since silanes are the major source for epitaxial growth of Si films, the surface of the film is covered by hydrogen.[4] Raman scattering and infrared absorption are known to be useful tools for probing hydrogen in Si; several scattering or absorption peaks were identified as $H_2$ molecules trapped at tetrahedral ($T_d$) sites or trapped by platelets, voids, point defects, etc.[1,5–9] Hydrogen terminates dangling bonds of vacancy-type defects,[8,9] and also interacts with interstitials.[10] Although intensive studies have been carried out, the interaction between hydrogen and process-induced defects is still unresolved because of the lack of techniques that are sensitive to the presence of point defects in the subsurface region. Positron annihilation is one established technique for investigating defects in semiconductors.[11] A slow/monoenergetic positron beam can be used to adjust the implantation profile of positrons in the region of interest in a sample by accelerating the positrons to a certain energy. In general, the incident energy of positrons varies from several electron volts to 30–50 keV, and the regions that can be sampled by such positrons can vary from the sample surface to depths of the order of microns. Defects introduced by hydrogen plasma or $H^+$ implantation have been investigated by this technique,[12–17] which showed that positrons are a useful probe for studying hydrogen-related defects in Si. The present study used a monoenergetic positron beam to investigate the H-terminated vacancies in $Si^+$-implanted Si.

When a positron is implanted into condensed matter, it annihilates with the electron and, emits two 511 keV $\gamma$ rays.[11] Those annihilation $\gamma$ rays are broadened by the momentum component of the annihilating electron–positron pair $p_L$, which is parallel to the direction of the $\gamma$ rays. The energy of the $\gamma$ rays is given by the relation $E_\gamma = 511 \pm \Delta E_\gamma$ keV. The Doppler shift, $\Delta E_\gamma$, is given by the relation $\Delta E_\gamma = p_L c/2$, where $c$ is the speed of light. A freely diffusing positron may be localized in a vacancy-type defect because of Coulomb repulsion from ion cores. Because the momentum distribution of electrons in such defects differs from that in bulk materials, these defects can be detected by measuring Doppler broadening spectra of annihilation radiation. The resultant change in the Doppler broadening spectra is characterized by the *S* parameter, which mainly reflects the change due to the annihilation of positron–electron pairs with a low momentum distribution. The lifetime of positrons trapped by vacancy-type defects increases because of the reduced electron density in such defects. Information obtained by measuring the lifetime spectra of positrons is also useful for identifying vacancy-type defects.[11]

## II. EXPERIMENT

The samples used in the present experiments were undoped Si(100) wafers (resistivity: >50 Ωcm) grown by the floating-zone (FZ) method. $Si^+$ ions were implanted at 200



Downloaded 23 Dec 2009 to 130.158.56.186. Redistribution subject to AIP license or copyright; see http://jap.aip.org/jap/copyright.jsp

keV up to a dose of $2\times10^{14}\,cm^{-2}$ at room temperature. This dosage is lower than the critical dose sufficient for creation of an amorphous region. The implanted samples were treated with atomic hydrogen at 190 °C for 30 min in a downstream region of hydrogen plasma. During this treatment, the samples were placed 60 cm from the plasma so that the activated species in the plasma do not damage the sample surface. This hydrogen-atom treatment (HAT) was also performed on the $Si^+$-implanted sample after being annealed at 435 °C. Raman scattering spectra of the samples were measured at room temperature. Details of the HAT and Raman measurements are described elsewhere.[7,8] After HAT, the samples were isothermally annealed in a $N_2$ atmosphere at 190–800 °C for 30 min.

A monoenergetic positron beam was used to measure the Doppler broadening spectra of annihilation radiation as a function of incident positron energy *E*. For each value of *E*, a spectrum with approximately $1\times10^6$ total counts was measured and characterized by the *S* parameter; the center region of the spectra was defined as $511\pm0.75$ keV. The relationship between *S* and *E* was analyzed by VEPFIT, a computer program developed by van Veen *et al.* [18] Details of the application of VEPFIT for ion-implanted Si are described elsewhere.[19] In the fitting procedure, the region sampled by positrons was divided into several blocks. VEPFIT was used to determine the fraction of positrons annihilated in each block and the corresponding *S* parameter. The $S-E$ curve was fit into the following equation:

$$S(E)=S_sF_s(E)+\sum_{i=1}^{n} S_iF_i(E), \qquad (1)$$

where $F_s(E)$ is the fraction of positrons annihilated at the surface and $F_i(E)$ is that in the *i*th block $[F_s(E)+\Sigma F_i(E)=1]$. $S_s$ and $S_i$ are the *S* parameters corresponding to, respectively, annihilation of positrons on the surface and that in the *i*th block. To determine the annihilation characteristic of positrons trapped by H-terminated vacancies, we used a coincidence-detection system[11] to obtain Doppler broadening spectra. The spectra were measured by a two-dimensional multichannel analyzer, and the diagonal cross section of the spectra was obtained with an energy width of 1.3 keV.

A pulsed monoenergetic positron beam was used to obtain the lifetime spectra of positrons.[20] Approximately $1\times10^6$ counts were accumulated for each lifetime spectrum. The lifetime spectrum of positrons, $S_{LT}(t)$, is given by

$$S_{LT}(t)=\sum \lambda_i I_i \exp(-\lambda_i t), \qquad (2)$$

where $\lambda_i$ and $I_i$ are, respectively, the annihilation rate of positrons of the *i*th component and their intensity. The lifetime of positrons, $\tau_i$, is given by $1/\lambda_i$. The lifetime spectra were analyzed with a time resolution (full width at half maximum) of approximately 250 ps by a computer program called RESOLUTION.[21]

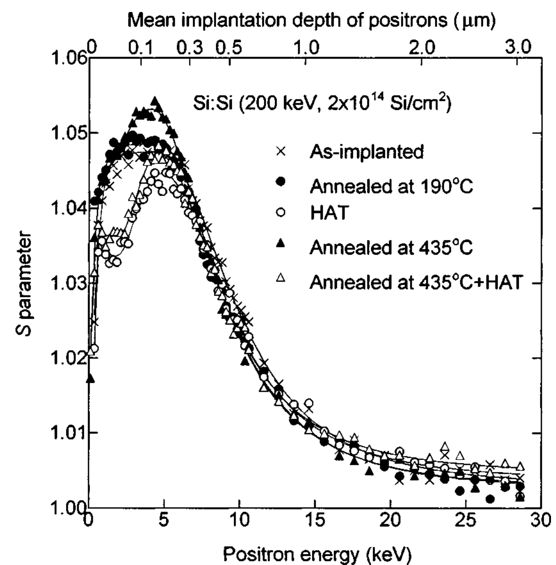


FIG. 1. *S* parameter as a function of incident positron energy *E* for $Si^+$−implanted Si before and after hydrogen atom treatment. Results for the samples annealed at 435 °C before HAT are also shown. For the samples after HAT, the valley observed in the $S-E$ curve ($E\cong2$ keV) is associated with the annihilation of positrons trapped by H-terminated vacancies. The solid curves are fits of Eq. (1) to the experimental data.

## III. RESULTS AND DISCUSSION

### A. Annihilation characteristic of positrons trapped by hydrogen-terminated vacancies

The *S* parameters of $Si^+$-implanted Si before and after HAT are shown in Fig. 1 as a function of *E*. The value of *S* was normalized to that for bulk Si. The corresponding mean implantation depth of positrons is shown on the upper horizontal axis. Figure 1 shows that *S* approaches a constant value at high $E(>25\,keV)$. This indicates that, in this energy range, almost all positrons annihilate in the substrate without diffusing back to the subsurface region. The observed increase in *S* at $E\cong4$ keV is due to the trapping of positrons by vacancy-type defects introduced by $Si^+$ implantation.[19] For the as-implanted sample, the lifetime spectrum of positrons was measured at $E=2$ keV, at which almost all positrons annihilate from the trapped state by defects. The spectrum was analyzed under the assumption of one annihilation mode, and the lifetime of positrons was obtained as 302 $\pm3$ ps. Since this lifetime is close to the calculated lifetime of positrons trapped by divacancies,[22,23] the mean size of the open volume of vacancy-type defects is close to that of divacancies. In the case of the sample that underwent HAT (hereafter referred to as the HAT sample), the value of *S* at $E\cong2$ keV was found to be smaller than that of the as-implanted sample. The observed decrease in *S*, therefore, can be attributed to the interaction between vacancy-type defects and hydrogen. The decrease in *S* due to HAT was also observed in the case of the sample annealed at 435 °C, which is higher than the annealing temperature of divacancies in Si (200–250 °C).[24] Since ion implantation introduces a variety of defects, no large change in the value of *S* before or after annealing out the divacancies was observed.[19,25]

Downloaded 23 Dec 2009 to 130.158.56.186. Redistribution subject to AIP license or copyright; see http://jap.aip.org/jap/copyright.jsp

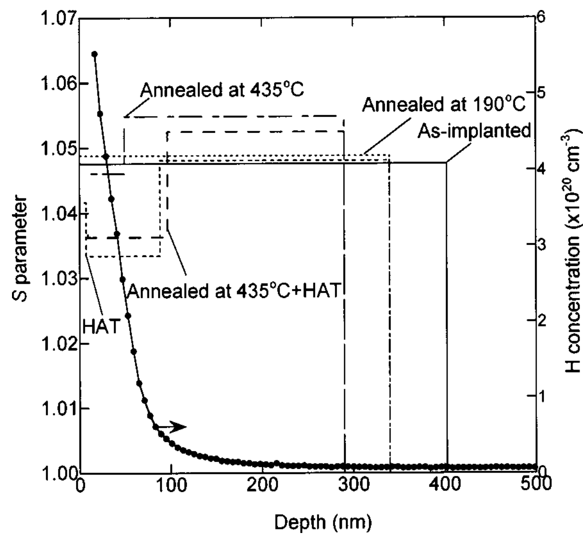


FIG. 2. Depth profiles of $S$ for $Si^+$-implanted Si before and after HAT obtained from analysis of the $S-E$ curves in Fig. 1. A depth profile of hydrogen measured by SIMS is also shown.

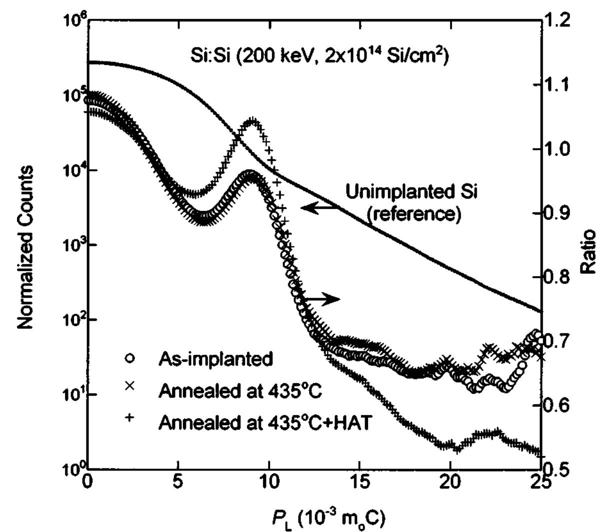


FIG. 3. Doppler broadening spectrum of positrons annihilated from the free state in Si (used as a reference). Ratio curves of Doppler broadening spectra for the samples before and after annealing at 435 °C and the HAT sample are also shown; each curve corresponds to the annihilation of positrons trapped by vacancy-type defects or H-terminated defects.

The $S-E$ curves shown in Fig. 1 were fit using VEPFIT. In the fitting procedure, the region sampled by the positrons was divided into two, three, or four blocks. The diffusion length of positrons, $L_d$, in the block located in the deepest region was fixed to $L_d$ for defect-free Si (200 nm).[19,26] This means that the trapping of positrons by defects in this block is negligible. The solid curves shown in Fig. 1 are the results of fit. The value of $L_d$ in the first block, $L_{d1}$, was derived as about 5 nm. This short diffusion length of positrons suggests that almost all positrons implanted into the first block annihilate from the trapped state.[19] Thus, $S_1$ is considered to be the characteristic value of $S$ for the annihilation of positrons trapped by defects in the first block. In the fitting procedure, it was assumed that $L_d$ in the blocks below the first one (except the deepest block) is the same as $L_{d1}$. Since the $S-E$ curves are represented well by this model, the derived value of $S_i$ is likely to be related to the annihilation of positrons trapped by defects in the $i$th block.

The depth distributions of $S$ obtained are shown in Fig. 2. Using secondary ion mass spectroscopy (SIMS), we measured the depth distribution of hydrogen in the as-implanted HAT sample, and the result is also shown in Fig. 2. After 190 °C annealing, the damaged region shifts toward the surface, but $S_1$ does not significantly change. The value of $S$ increases after annealing at 435 °C, suggesting clustering of vacancy-type defects. For the as-implanted sample after HAT, the region with a small value of $S$ (10–100 nm) matches the depth distribution of hydrogen. This suggests that HAT decreases the characteristic value of $S$ in the damaged region. The same is true for the sample annealed at 435 °C.

To interpret the change in Doppler broadening spectra by HAT, the ratio of the coincidence spectra was calculated. Figure 3 plots the Doppler broadening spectrum that corresponds to positron annihilation from the free state on the left-hand axis; the horizontal axis shows $p_L$ ($m_0$ is the rest of the mass of an electron). It can be seen that the spectrum mainly consists of a narrow and a broad component. The broad component observed at $p_L > 10\times10^{-3}\,m_0c$ corresponds to the annihilation of positrons with core electrons. This spectrum can be used as a reference. The ratio of the Doppler broadening spectrum measured at $E=2$ keV for the sample before and after annealing at 435 °C and the sample after HAT to the reference spectrum is plotted on the right-hand axis in Fig. 3. The overall behavior of the ratio curves for the sample before annealing is similar to that reported by Tang and co-workers.[27,28] According to Tang and co-workers,[27,28] the origin of the pronounced peak around $9\times10^{-3}\,m_0c$ is slowly varying momentum density of dangling-bond electrons over rapidly decreasing momentum density around the Jones zone boundary of Si.

In Fig. 3, the intensity of the peak around $9\times10^{-3}\,m_0c$ increased after HAT. Using a full-potential and all-electron first-principles method, Tang *et al.* [27] calculated Doppler broadening profiles for Si containing oxygen-vacancy complexes. They found that the intensity of the peak around $9\times10^{-3}\,m_0c$ becomes significant with an increase in the number of oxygen atoms coupled with divacancies. This was attributed to the fact that the dangling-bond wave functions dominated by oxygen atoms are more localized than those dominated by Si atoms.[27,28] In the present experiment, therefore, the observed increase in peak intensity can also be attributed to the annihilation of positrons with electrons localized in vacancy-type defects, and such electrons are introduced by coupling of the defects and hydrogen atoms. This causes a decrease in the annihilation probability of positron–electron pairs with a low-momentum distribution ($p_L=0$), and results in a decrease in the $S$ value. Raman studies have revealed that HAT produces several Raman lines around $2000\,\text{cm}^{-1}$, which were identified as H-terminated open volumes.[1,8,9] Those results also support the above discussion.

After HAT, the ratio in the high momentum region ($>15\,m_0c$) is smaller than that before HAT. The effect of

Downloaded 23 Dec 2009 to 130.158.56.186. Redistribution subject to AIP license or copyright; see http://jap.aip.org/jap/copyright.jsp

HAT on the ratio curves of the as-implanted sample without pre-annealing was identical to that on the pre-annealed sample. According to the calculation,[27] major electrons annihilate with positrons in this region are 2*p* and 2*s* core electrons of Si. In H-decorated vacancies, a positron is likely to be localized at the center of the open volume because of the repulsion between a positron and hydrogen atoms, and this could be the origin of the observed decrease in the annihilation probability of positrons with core electrons of Si atoms. For the sample annealed at 435 °C, after HAT, the lifetime of positrons at $E=2$ keV was $324\pm1$ ps. Because the lifetime of positrons trapped by defects is longer than that for divacancies, the electron density in the defects is lower than that in divacancies. The decrease in $S$ due to HAT, therefore, cannot be attributed to the decrease in the open volume of the defects due to H decoration. To more fully understand the annihilation characteristic of positrons trapped by H-terminated defects, it is necessary to perform further experiments and theoretical calculations on the momentum distribution of electrons in such defects.

Asoka-Kumar *et al.* [14] and Schut *et al.* [17] reported that effect of HAT on the $S$ value for Si without ion implantation, and they found an increase in the value of $S$ near the surface. This was attributed to the trapping of positrons by voids or nanocavities introduced by HAT. In the present experiments, since hydrogen atoms were introduced into the $Si^+$-implanted sample, the interaction between hydrogen and pre-existing multivacancies suppresses the formation of voids or nanocavities.[29] Platelets (or amorphous phase) are likely to be introduced into the region containing a very high concentration of hydrogen. As shown in Fig. 2, however, the second block (depth: 10–100 nm) is deeper than the depth at which the hydrogen concentration peaks appear. In the present experiments, the effect of the trapping of positrons by platelets on the $S$ value cannot be completely neglected, but major defects produce a small $S$ value (second block) are considered to be H-terminated vacancies.

### B. Annealing behavior of hydrogen-terminated vacancies

The as-implanted and HAT samples were isochronally annealed in the temperature range between 190 and 800 °C. Figure 4 shows the $S-E$ curves for the samples annealed at 385–700 °C. For the sample without HAT, after annealing at 385 °C, the $S-E$ curve observed is similar to that for the as-implanted sample (Fig. 1). In the case of annealing at 490 °C, the value of $S$ at $E\cong2$ keV decreased, suggesting a decrease in the concentration or the size of the open volume of vacancy-type defects in the subsurface region. The damaged region shifts towards the surface after annealing at 600 °C, and because of the clustering of defects, the value of $S$ in the subsurface region increased. After annealing at 700 °C, a decrease in the $S$ value at $E=2-3$ keV was observed, suggesting that almost all defects introduced by implantation were annealed out. With regard to the HAT sample, after annealing at 385 °C, the influence of the H termination of vacancies on $S$ is clearly seen. After being annealed at 490 °C, the defects located in the deeper region (defects without H termination) were annealed out. In the case of annealing at 600 and 700 °C, the $S-E$ curves for the HAT sample are almost identical to those for the non-HAT sample. Figure 5 summarizes the annealing behavior of the $S$ value at $E=2$ keV for the samples before and after HAT.

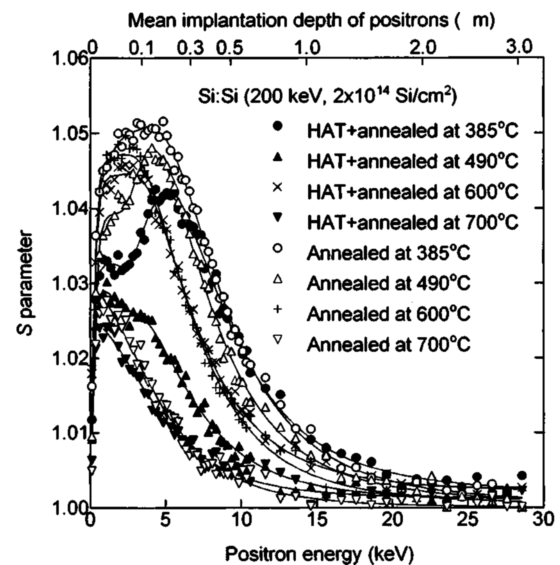


FIG. 4. $S-E$ curves for $Si^+$-implanted Si annealed at 385–700 °C. For the HAT sample, the difference in the values of $S$ observed after annealing at 490 and 600 °C was attributed to the release of hydrogen from vacancy-type defects at 600 °C annealing. The solid curves are fits of Eq. (1) to the experimental data.

Figure 6 shows Raman spectra for the HAT sample after annealing at various temperatures. The vibrational line at 3820 $cm^{-1}$, which is attributed to $H_2$ molecules trapped by H-terminated vacancies or those adjacent to such defects,[8] disappeared after annealing at 280 °C. The positron annihilation parameters, however, did not significantly change after annealing at this temperature. Thus, positrons are unlikely to be trapped by defects containing $H_2$ molecules. After annealing above 600 °C, all the Raman peaks arising from $H_2$ and

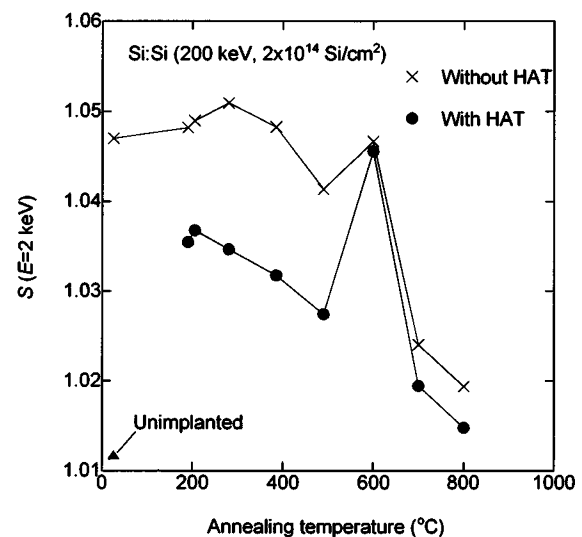


FIG. 5. Annealing behavior of the value of $S$ at $E=2$ keV for $Si^+-$implanted Si with and without HAT.

Downloaded 23 Dec 2009 to 130.158.56.186. Redistribution subject to AIP license or copyright; see http://jap.aip.org/jap/copyright.jsp

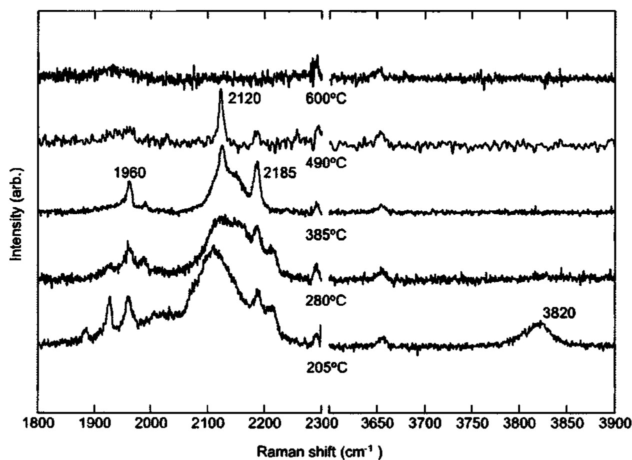


FIG. 6. Raman spectra for $Si^+$-implanted Si with HAT. The vibrational line at $3820\,cm^{-1}$ is due to $H_2$ molecules trapped by H-terminated vacancies or those adjacent to such defects (see Ref. 8). Several Raman lines observed at $1850-2250\,cm^{-1}$ are associated with Si–H bonds.

Si–H bonds disappeared. Thus, the increase in the value of $S$ after annealing at 600 °C can be attributed to the release of hydrogen from vacancy-type defects.

For the $S-E$ curves obtained, analysis similar to that described in Sec. III A was performed. For the sample before HAT, the location between the damaged region and the defect-free region, $D_{1/2}$, was 360 nm, and it starts to shift towards the surface with annealing at 490 °C (the value of $D_{1/2}$ for the sample annealed at 600 °C was 150 nm). For the HAT sample, after being annealed at 490 °C, the region of "pure" vacancies disappeared, and the region of H-terminated defects was 0–160 nm. In the case of annealing at 600 °C, the position of the interface between the damaged and defect-free regions agrees with that in the non-HAT sample.

Using similar samples used in the present experiments, the annealing behavior of Raman spectra for $Si^+$-implanted Si after HAT was reported by Mori *et al.* [29] In their experiments, after annealing at 610 °C (for 30 min), the sample was hydrogenated again. After this rehydrogenation, a vibrational line was observed at around $3820\,cm^{-1}$. The present experiments suggest that, after the release of hydrogen, vacancy-type defects still exist even after 600 °C annealing. Thus, the line at $3820\,cm^{-1}$ can be attributed to $H_2$ trapped by residual defects. In Fig. 6, the lines observed at 1960 and $2185\,cm^{-1}$ disappeared after annealing at 490 °C. At this annealing temperature, the pure vacancies located below the region of H-terminated vacancies were annealed out. The migration of Si atoms caused by the annealing out of such defects could change the configuration of atoms near Si–H bonds corresponding to 1960 and $2185\,cm^{-1}$.

## IV. SUMMARY

Hydrogen-terminated vacancies in $Si^+$-implanted FZ Si were investigated. After ion implantation into Si samples, hydrogen atoms were introduced as neutral atoms by HAT. A monoenergetic positron beam was used to obtain Doppler broadening spectra of the annihilation radiation as a function of the incident positron energy. A pulsed monoenergetic positron beam was used to obtain the lifetime spectra of positrons. The value of the line shape parameter, $S$, was increased by ion implantation, suggesting the annihilation of positrons trapped by vacancy-type defects; the mean size of the open volume of such defects was close to that of divacancies. It was found that HAT decreases the value of $S$ corresponding to the annihilation of positrons in the subsurface region (depth: 10–100 nm). The depth profile of hydrogen atoms measured by SIMS agrees well with the region in which the value of $S$ is small. Measurements of the Raman spectra show several vibrational lines that correspond to Si–H bonds. Thus, the decrease in $S$ is attributed to the annihilation of positrons trapped by H-terminated vacancies. The origin of the decrease in $S$ is the increase in the annihilation probability of positrons with localized electrons in H-decorated multivacancies.

Isochronal annealing experiments were performed in the temperature range of 205–800 °C. It was found that $S$ did not significantly change after annealing below 385 °C, but after annealing at 490 °C, almost all vacancy-type defects located below the H-rich region were annealed out. Annealing at 600 °C results in similar $S-E$ curves for both the samples with and without HAT. These results were in good agreement with the thermal behavior of the Raman spectrum which suggests the release of hydrogen from vacancy-type defects at 600 °C. The present results show that a monoenergetic positron beam can be used to study the behavior of hydrogen in Si. The potential of positron annihilation for detecting H-terminated vacancies located in the subsurface region and that of Raman spectroscopy for identifying various Si–H stretching modes makes these techniques a powerful tool for studying the correlation between hydrogen and process-induced defects.

[1] *Hydrogen in Semiconductors*, edited by J. I. Pankove and N. M. Johnson (Academic, New York, 1991).
[2] A. J. Auberton-Hervé, M. Bruel, B. Aspar, C. Maleville, and H. Moriceau, IEICE Trans. Electron. **E80-C**, 358 (1997).
[3] K. Sakaguchi, N. Sato, K. Yamagata, T. Atoji, Y. Fujiyama, J. Nakayama, and T. Yonehara, IEICE Trans. Electron. **E80-C**, 378 (1997).
[4] T. Hashizume, S. Heike, M. Lutwyche, S. Watanabe, K. Nakajima, T. Nishi, and Y. Wada, Jpn. J. Appl. Phys., Part 2 **35**, L1085 (1996).
[5] C. G. Van de Walle, Phys. Rev. Lett. **80**, 2177 (1998).
[6] B. Hourahine, R. Jones, S. Öberg, R. C. Newman, P. R. Beriddon, and E. Roduner, Phys. Rev. B **57**, R12666 (1998).
[7] K. Ishioka, M. Kitajima, S. Tateishi, K. Nakanoya, N. Fukata, T. Mori, K. Murakami, and S. Hishita, Phys. Rev. B **60**, 10852 (1999).
[8] K. Murakami, K. Ishioka, M. Kitajima, S. Tateishi, K. Nakanoya, T. Mori, and S. Hishita, Physica B **273–274**, 188 (1999).
[9] T. Akiyama and A. Oshiyama, J. Phys. Soc. Jpn. **70**, 1627 (2001).
[10] C. G. Van de Walle and J. Neugebauer, Phys. Rev. B **52**, R14320 (1995).
[11] R. Krause-Rehberg and H. S. Leipner, *Positron Annihilation in Semiconductors*, Solid-State Sciences Ser. 127 (Springer, Berlin, 1999).
[12] J. Keinonen, *et al.* Phys. Rev. B **37**, 8269 (1988).
[13] R. S. Brusa, M. Duarte Naia, A. Zecca, C. Nobili, G. Ottaviani, R. Tonini, and A. Dupasquier, Phys. Rev. B **49**, 7271 (1994).
[14] P. Asoka-Kumar, H.J. Stein, and K.G. Lynn, Appl. Phys. Lett. **64**, 1684 (1994).
[15] M. Fujinami, R. Suzuki, T. Ohdaira, and T. Mikado, Phys. Rev. B **58**, 12559 (1998).

Downloaded 23 Dec 2009 to 130.158.56.186. Redistribution subject to AIP license or copyright; see http://jap.aip.org/jap/copyright.jsp

[16] C. E. Gonzalez, S. C. Sharma, N. Hozhabri, D. Z. Chi, and S. Ashok, Appl. Phys. A: Mater. Sci. Process. **68**, 643 (1999).
[17] H. Schut, A. van Veen, S. W. H. Eijt, R. Job, A. G. Ulyasin, and W. R. Fahrner, Nucl. Instrum. Methods Phys. Res. B **186**, 94 (2002).
[18] A. van Veen, H. Schut, J. de Vries, R. A. Hakvoort, and M. R. Ijpma, AIP Conf. Proc. **218**, 171 (1990).
[19] A. Uedono, T. Kitano, K. Hamada, T. Moriya, T. Kawano, S. Tanigawa, R. Suzuki, T. Ohdaira, and T. Mikado, Jpn. J. Appl. Phys., Part 1 **36**, 2571 (1997).
[20] R. Suzuki, T. Ohdaira, and T. Mikado, Radiat. Phys. Chem. **58**, 603 (2000).
[21] P. Kirkegaard, M. Eldrup, O. E. Mogensen, and N. J. Pedersen, Comput. Phys. Commun. **23**, 307 (1981).
[22] M. J. Puska and C. Corbel, Phys. Rev. B **38**, 9874 (1988).
[23] M. Saito and A. Oshiyama, Phys. Rev. B **53**, 7810 (1996).
[24] J. W. Corbett, J. P. Karins and T. Y. Tan, Nucl. Instrum. Methods Phys. Res. **182/183**, 457 (1981).
[25] A. Uedono, Y. Ujihira, A. Ikari, H. Haga, and O. Yoda, Hyperfine Interact. **79**, 615 (1993).
[26] A. Uedono, M. Watanabe, S. Takasu, T. Sabato, and S. Tanigawa, J. Phys.: Condens. Matter **12**, 719 (2000).
[27] Z. Tang, T. Nonaka, Y. Nagai, and M. Hasegawa, Mater. Sci. Forum **363–365**, 67 (2001).
[28] M. Hasegawa, Z. Tang, Y. Nagai, T. Nonaka, and K. Nakamura, Surf. Sci. **194**, 76 (2002).
[29] T. Mori, K. Otsuka, N. Umehara, K. Ishioka, M. Kitajima, S. Hishita, and K. Murakami, Physica B **302–303**, 239 (2001).

Downloaded 23 Dec 2009 to 130.158.56.186. Redistribution subject to AIP license or copyright; see http://jap.aip.org/jap/copyright.jsp